

Mutations of a Redundant α -Tubulin Gene Affect *Caenorhabditis elegans* Early Embryonic Cleavage via MEI-1/Katanin-Dependent and -Independent Pathways

Chenggang Lu and Paul E. Mains¹

Genes and Development Research Group, Department of Biochemistry and Molecular Biology,
University of Calgary, Calgary, Alberta T2N 4N1, Canada

Manuscript received April 15, 2004

Accepted for publication February 9, 2005

ABSTRACT

The *C. elegans* zygote supports both meiosis and mitosis within a common cytoplasm. The meiotic spindle is small and is located anteriorly, whereas the first mitotic spindle fills the zygote. The *C. elegans* microtubule-severing complex, katanin, is encoded by the *mei-1* and *mei-2* genes and is solely required for oocyte meiotic spindle formation; ectopic mitotic katanin activity disrupts mitotic spindles. Here we characterize two mutations that rescue the lethality caused by ectopic MEI-1/MEI-2. Both mutations are gain-of-function alleles of *tba-2* α -tubulin. These *tba-2* alleles do not prevent MEI-1/MEI-2 microtubule localization but do interfere with its activity. TBA-1 and TBA-2 are redundant for viability, but when katanin activity is limiting, TBA-2 is preferred over TBA-1 by katanin. This is similar to what we previously reported for the β -tubulins. Removing both preferred α - and β -isoforms results in normal development, suggesting that the katanin isoform preferences are not absolute. We conclude that while the *C. elegans* embryo expresses redundant α - and β -tubulin isoforms, they nevertheless have subtle functional specializations. Finally, we identified a dominant *tba-2* allele that disrupts both meiotic and mitotic spindle formation independently of MEI-1/MEI-2 activity. Genetic studies suggest that this *tba-2* mutation has a “poisonous” effect on microtubule function.

THE eukaryotic microtubule cytoskeleton is involved in a variety of processes, including cell division, intracellular transport, cell shape maintenance, and cell motility. Despite their diverse cellular functions, microtubule arrays are always polymers of α - and β -tubulin heterodimers. Microtubules are not static structures, and their dynamic properties vary both temporally and spatially to fulfill different functional requirements (MITCHISON 1989; ZHAI *et al.* 1996). A critical feature of microtubule dynamics is its ability to switch between growing (polymerizing) and rapidly shrinking (catastrophic) states, a property known as dynamic instability (MITCHISON and KIRSCHNER 1984). The dynamic instability of microtubules arises partly from the intrinsic properties of α - and β -tubulins; previous structure-function studies showed that tubulin mutations affect microtubule dynamics both *in vivo* and *in vitro* (ANDERS and BOTSTEIN 2001; DOUGHERTY *et al.* 2001). Microtubule dynamics are also regulated by the presence of stabilizing and destabilizing factors (DAVIS *et al.* 1994; DESAI and MITCHISON 1997). For example, microtubule-associated proteins (MAPs), microtubule destabilizers, and

microtubule motor proteins were shown to regulate microtubule dynamics in a variety of systems (MCNALLY and VALE 1993; VASQUEZ *et al.* 1994; TRINCZEK *et al.* 1995; HUNTER *et al.* 2003).

Almost all organisms have multiple α - and β -tubulin isotypes (LUDUEÑA 1998). Within an organism, each cell type normally expresses more than one family member, and these are often modified post-translationally (LUDUEÑA 1998; XIA *et al.* 2000). Conservation of different isotypes across species suggests natural selection for isotype-specific functions (WILSON and BORISY 1997). Several *in vitro* studies have demonstrated that different tubulin isotypes affect microtubule dynamics and drug sensitivity (PANDA *et al.* 1994; DERRY *et al.* 1997; BODE *et al.* 2003). Previous *in vivo* studies focused mostly on tissue-specific isotypes. For example, *Drosophila* testis specifically expresses a $\beta 2$ isotype that is required for proper axoneme organization and function (HOYLE and RAFF 1990). Likewise, *Caenorhabditis elegans* mechanosensory neurons express a specific pair of α - and β -tubulins that confer distinctive protofilament organization and microtubule function (SAVAGE *et al.* 1989; FUKUSHIGE *et al.* 1999).

The *C. elegans* embryo expresses pairs of closely related α - and β -tubulins that are largely redundant for normal development (WRIGHT and HUNTER 2003; LU *et al.* 2004; PHILLIPS *et al.* 2004). Gain-of-function (*gf*) mutants of the α -tubulin gene *tba-1* and the β -tubulin

¹Corresponding author: Genes and Development Research Group, Department of Biochemistry and Molecular Biology, 3330 Hospital Dr. NW, University of Calgary, Calgary, Alberta T2N 4N1, Canada. E-mail: mains@ucalgary.ca

gene *tbb-2* disrupt spindle organization and function, and these mutations likely act by interfering with the function of the α - or β -gene isotypes of both respective tubulins (WRIGHT and HUNTER 2003; ELLIS *et al.* 2004; PHILLIPS *et al.* 2004). Loss-of-function (*lf*) analysis revealed relatively minor developmental defects associated with diminishing one isotype of each pair, but simultaneous loss of both members of a pair was lethal (WRIGHT and HUNTER 2003; LU *et al.* 2004; PHILLIPS *et al.* 2004). These results suggest functional redundancy of α - and β -isotypes, at least at a superficial level. However, we recently demonstrated functional differences between the two embryonic *C. elegans* β -tubulins, TBB-1 and TBB-2: while either is sufficient for wild-type development, TBB-2 interacts preferentially with MEI-1 and MEI-2, the subunits of the worm katanin microtubule-severing complex (see below) (LU *et al.* 2004).

The microtubule-severing complex katanin is an example of a MAP that influences microtubule function and dynamics (McNALLY and VALE 1993). MEI-1 and MEI-2, which encode the subunits of *C. elegans* katanin, are specifically required for female meiotic spindle formation. Meiotic spindles form after fertilization of the worm embryo in the same cytoplasm that later supports embryonic mitosis (ALBERTSON 1984; KEMPHUES *et al.* 1986; SRAYKO *et al.* 2000). Meiotic spindle formation requires MEI-1/MEI-2 microtubule-severing activity, but proper spindle formation during subsequent mitosis requires postmeiotic degradation of MEI-1/MEI-2 (CLARK-MAGUIRE and MAINS 1994a; KURZ *et al.* 2002; FURUKAWA *et al.* 2003; PINTARD *et al.* 2003; XU *et al.* 2003). Ectopic presence of MEI-1/MEI-2-severing activity in mitosis results in small, misoriented spindles (CLARK-MAGUIRE and MAINS 1994a; DOW and MAINS 1998; SRAYKO *et al.* 2000), resembling those seen after treating embryos with the microtubule-destabilizing drug nocodazole (STROME and WOOD 1983; HYMAN and WHITE 1987).

In this work, we report two types of mutations in the *tba-2* α -tubulin gene that affect microtubule dynamics. Two alleles result in microtubules that are resistant to MEI-1/MEI-2 activity while a third mutation results in short microtubules independent of MEI-1/MEI-2 function and likely acts as a neomorph that interferes with both *tba-2* and *tba-1* function. In addition, as with the two superficially redundant β -tubulins described above (LU *et al.* 2004), the two redundant α -tubulins interact differentially with MEI-1/MEI-2. Simultaneous loss of any combination of one member of each α - or β -tubulin isotype is viable.

MATERIALS AND METHODS

Nematode strains and culture conditions: *C. elegans* (var. Bristol) was cultured under standard conditions (BRENNER 1974) and brood analysis was done as described by MAINS *et al.* (1990b). Hatching rates were scored among 500–2500 embryos except when otherwise indicated. For all temperature-sensitive (*ts*) alleles, hermaphrodites were raised at 15°

and shifted to higher temperatures as L4 larvae for brood analyses.

The following genes and alleles were used: LG I, *lin-11* (*n566*), *unc-13*(*e1092*), *unc-29*(*e1072*), *mei-1*(*ct46gf*), *mei-2*(*ct98*), *daf-8*(*e1393*), *unc-101*(*m1*), *tba-2*(*sb25*, *sb27*, *sb51*, *sb51sb116*, and *sb51sb117*), *unc-59*(*e261*), and the chromosomal deficiency *dxDf2*; LG II, *zyg-9*(*b244*); LG III, *tbb-2*(*sb26*, *gk129*, and *gk130*), *tbb-1*(*gk207*), *dpy-17*(*e164*). Descriptions of these genes are found at Wormbase (<http://www.wormbase.org>). The chromosomal translocation *hT2* and chromosome I inversion *hInI* (ZETKA and ROSE 1992) were used as balancers. CB4856 was used to provide polymorphisms for single nucleotide polymorphism (SNP) mapping (WICKS *et al.* 2001).

Because most of the tubulin alleles used in this study have either no or minor phenotypes by themselves, strain construction made use of linked morphological markers. However, nearly all morphological markers from the final double or triple mutants were removed from strains to avoid nonspecific background effects. Every strain listed in the tables was DNA sequenced to confirm the continued presence of all intended tubulin alleles. Outcrossing of *tbb-1* and *tbb-2* deletion alleles from the *C. elegans* Knockout Consortium was done as previously described (LU *et al.* 2004).

Genetic mapping and cloning: *mei-1*(*ct46gf*) results in dominant, *ts* maternal-effect lethality (MAINS *et al.* 1990a). *sb25* and *sb27* were selected as suppressors of this mutation in the screen described in CLANDININ and MAINS (1993). Both *sb25* and *sb27* were genetically mapped to the region between *unc-101* and *unc-59* on LG I: *mei-1*(*ct46*) *unc-29* *sb25* males were crossed to *unc-101* *unc-59*. *Unc-29* homozygotes were selected from their progeny (*unc-29* *mei-1*(*ct46*) *sb25*?/*unc-101*? *unc-59*?). Hatching rates were scored at the semirestrictive temperature of *mei-1*(*ct46*), 20°, where *sb25*/*sb25*, *sb25*/+, and +/+ can be distinguished (57%, 12%, and 1.5% hatching, respectively). Among those still homozygous for *mei-1*(*ct46*), seven segregated *unc-101* *unc-59*, and all of these were heterozygous for *sb25*. Nine segregated only *unc-59*, of which five were heterozygous and four were homozygous for *sb25*, which placed *sb25* between *unc-101* and *unc-59*. These data were confirmed by three-factor mapping where *unc-101* *unc-59* recombinants were collected from *unc-101* *sb25* +/+ + *unc-59* heterozygotes. Each recombinant was crossed with *mei-1*(*ct46*) *unc-29* *sb25* males to test for suppressor homozygosity in the outcross progeny. Of 18 recombinants, 12 lost *sb25* during recombination and 6 retained *sb25*. A three-factor map was generated similarly for *sb27* (data not shown).

Within the *unc-101* *unc-59* region, SNP mapping (WICKS *et al.* 2001) further defined the location of *sb25*. *unc-101* *sb25* *unc-59* hermaphrodites were crossed to CB4856 (Hawaiian) males and *Unc-101* non-*Unc-59* F₂ recombinants were allowed to produce a few progeny before crossing with *mei-1*(*ct46*) *unc-29* *sb25* males. For each recombinant, hatching rates were scored from 10 outcross progeny to test for *sb25* homozygosity or heterozygosity. The self-progeny produced by each *Unc-101* non-*Unc-59* recombinant prior to crossing were then examined for the presence of various SNP makers within the region. This gave the map order F08A8:3890 (8) *sb25* (7) Y26D4A:7397, where the number of crossovers in each region is denoted within parentheses. This corresponds to four overlapping cosmids or 129 kbp on the physical map. This region includes two predicted candidates, *pbs-2* (C47B2.2) and *tba-2* (C47B2.3). Sequencing of candidate genomic sequences from *sb25* and *sb27* was performed as described (SRAYKO *et al.* 2000). At least two independent PCR products were sequenced to avoid PCR-generated errors; both mutations resulted in changes within *tba-2* only.

The dominant *ts* maternal-effect lethal mutation *sb51* was originally isolated as described by MITENKO *et al.* (1997). We previously reported a 70% embryonic lethality associated with

sb51 homozygotes at 15° (MITENKO *et al.* 1997). However, further examination of the strain (following further outcrossing) revealed that homozygous *sb51* adults showed a fully penetrant sterility at all temperatures. *sb51* was SNP mapped using its homozygous sterile phenotype. From *sb51 unc-59*/Hawaiian heterozygotes, sterile Unc-59 adults were scored for SNP markers, placing *sb51* between F08A8:3890 and *unc-59* (data not shown). This is the same region where *sb25* and *sb27* mapped, and *tba-2* genomic sequence was amplified from *sb51* homozygotes and sequenced as described above.

Isolation of intragenic revertant of *tba-2(sb51)*: Balanced *tba-2(sb51) unc-59/hT2* heterozygotes were mutagenized with ethyl methanesulfonate (Sigma, St. Louis) as described by BRENNER (1974). Two to five mutagenized hermaphrodites were transferred to individual plates and allowed to self at 15°. Revertants were isolated by upshifting the F₁ larvae to 25° and selecting plates with many viable progeny and fertile Unc-59 adults. Two intragenic revertants, *sb116* and *sb117*, were found among 12,500 haploid genomes (the screen was inefficient because crossover suppression by *hT2* in the *tba-2 unc-59* region is not complete and because so many positive plates contained crossovers rather than the desired revertants). Sequencing of the *tba-2* gene in *sb116* and *sb117* was performed on fertile homozygotes as described above. *sb116* was outcrossed three times before further analysis.

Microscopy and immunofluorescence: L4 or younger animals were upshifted to 25° overnight before fixation or mounting. Living embryos were dissected from gravid hermaphrodites in 25° egg buffer (EDGAR and MCGHEE 1986) and mounted on slides with a 3% agar pad. Nomarski time-lapse recording was performed using a Zeiss Axioplan 2 microscope with AxioVision software. For immunofluorescence, embryos were freeze cracked and fixed with methanol-acetone as described by KEMPHUES *et al.* (1986). Cold-induced microtubule destabilization was performed before freeze crack as described by HANNAK *et al.* (2002). Embryos were expelled from hermaphrodites on a polylysine-coated slide by applying gentle pressure on a coverslip. Slides were then placed on an ice-water-bathed aluminum block for 0, 5, and 8 min (in both of two separate experiments) before fixation and were stained to visualize microtubules and DNA. MEI-1 and MEI-2 antibodies were used as described (SRAYKO *et al.* 2000). α -Tubulin localization was determined with the mouse DM 1A α -tubulin monoclonal antibody (Sigma) at 1/200 dilution. Secondary antibodies (Jackson ImmunoResearch, West Grove, PA) used were FITC-conjugated goat anti-rabbit (1/50) and Texas red-conjugated goat anti-mouse (1/100). DNA was visualized with 4',6-diamidino-2'-phenylindole dihydrochloride as described by SRAYKO *et al.* (2000). Photographs were taken with a Hamamatsu ORCA-ER digital camera and deconvolved using Zeiss AxioVision software.

RNAi: *tbb-1* and *tbb-2* RNA interference (RNAi) was performed as described in LU *et al.* (2004) using the gene-specific C-terminal and 3'-UTR regions. Similar gene-specific *tba-1* and *tba-2* RNAi constructs (PHILLIPS *et al.* 2004) were kindly provided by J. Phillips and B. Bowerman (University of Oregon). RNA was transcribed using the MEGAscript system (Ambion, Austin, TX), and DNA templates were digested with DNase I. The resulting RNAs were purified and annealed for injection as described by A. Fire (<ftp://ciwemb.edu/PNF/byName:/FireLabWeb/>). Embryos from injected hermaphrodites were dissected for mounting 24 hr postinjection. *zyg-9* RNAi was performed using a feeding construct included in the *C. elegans* chromosome I RNAi feeding library (FRASER *et al.* 2000).

RESULTS

A dominant mutation disrupts spindle function and interacts with members of the *mei-1* pathway: We first

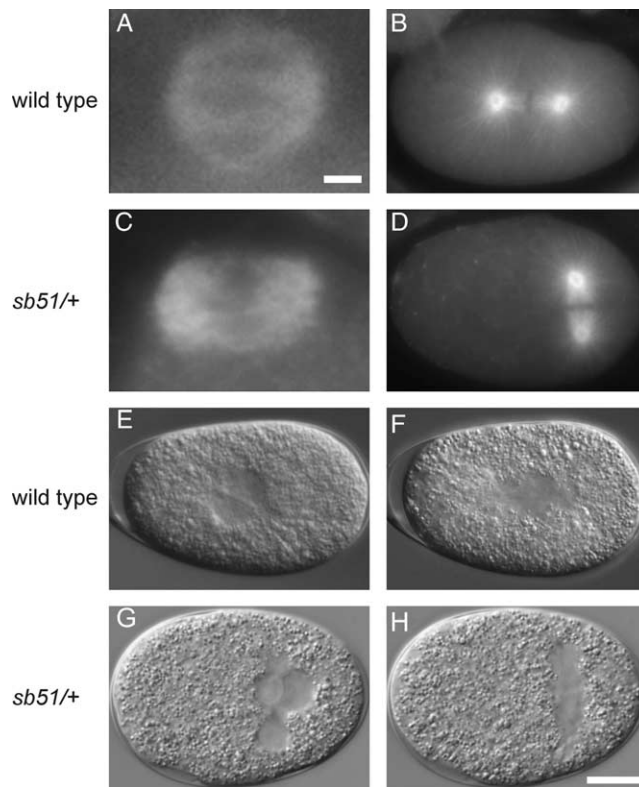


FIGURE 1.—Meiotic and mitotic phenotypes of embryos from *tba-2(sb51)/+* hermaphrodites at 25°. (A–D) α -Tubulin staining was used to visualize spindle structures. (E–H) Nomarski images of pronuclear fusion-stage embryos and embryos in their first mitosis. Meiotic spindle poles of mutant embryos (C) are not as well focused as wild type (A), and meiotic failure often leads to multiple maternal pronuclei (G) as compared to wild type (E). Mutant first mitotic spindles are always aligned on the transverse axis (D and H) and have short aster microtubules (D) as compared to wild type (B and F). Bars: 2 μ m in A; 10 μ m in H.

describe a dominant, *ts* maternal-effect lethal mutation, *sb51*, which results in dominant defects in both female meiosis and subsequent mitoses. *sb51* was isolated from a screen for dominant, *ts* maternal-effect lethal mutations and was previously assigned the gene name *mel-45* (MITENKO *et al.* 1997). Below, we demonstrate that *sb51* corresponds to the gene *tba-2*, and hereafter we use this designation. Embryos from *tba-2(sb51)/+* hermaphrodites are referred to as “mutant embryos.”

We analyzed embryos from heterozygous hermaphrodites grown at the nonpermissive temperature by Nomarski time-lapse video recording and tubulin immunolocalization to visualize spindle morphology. As shown in Figure 1, these embryos showed meiotic (7/11) and mitotic (15/15) spindle defects similar to those caused by mutations that reduce microtubule stability (MATTHEWS *et al.* 1998; SRAYKO *et al.* 2000; SEGBERT *et al.* 2003; WRIGHT and HUNTER 2003; ELLIS *et al.* 2004). In these embryos, female meiotic spindles are not organized well (Figure 1C), often resulting in abnormal polar-body extrusion (6/11) and multiple maternal pronu-

TABLE 1
***tba-2(sb51)* interacts with the *mei-1* pathway**

Maternal genotype	Embryonic hatching (%)	
	15°	20°
<i>tba-2(sb51)/+</i>	44	27
<i>mei-1(ct46gf)/+</i>	70	31
<i>mei-1(ct46gf) +/+ tba-2(sb51)</i>	0	0
<i>mel-26(ct61)/+</i>	94	0
<i>mel-26(ct61) +/+ tba-2(sb51)</i>	0.6	ND
<i>mei-2(ct98)/+</i>	ND	97
<i>mei-2(ct98) +/+ tba-2(sb51)</i>	ND	5.2

ND, not determined.

clei (5/11) at the stage of pronuclear migration (Figure 1G). The subsequent mitotic spindles are always (15/15) displaced from their normal position on the anterior-posterior axis and have smaller asters (Figure 1, D and H). Adult *tba-2(sb51)* homozygotes are sterile, and their germlines have no mature oocytes and very few pachytene-stage nuclei (data not shown).

The *C. elegans mei-1* and *mei-2* genes encode the homologs of the microtubule-severing complex katanin and are specifically required for meiotic spindle formation (SRAYKO *et al.* 2000). MEI-1/MEI-2 activity is downregulated immediately after meiosis to ensure normal mitotic spindle formation; failure to do so in *mel-26* mutants, the gene that normally inhibits *mei-1* postmeiotic activity, or *mei-1(ct46gf)*, which is refractory to postmeiotic *mel-26* inhibition, results in mitotic spindle defects (CLARK-MAGUIRE and MAINS 1994a; DOW and MAINS 1998; SRAYKO *et al.* 2000). *tba-2(sb51)* genetically interacts with all genes in this pathway (Table 1 and data not shown). *sb51* dominantly enhanced both *mei-1(ct46gf)* and *mel-26(ct61)* (Table 1, lines 1–5). *sb51* also strongly enhanced a *mei-2* hypomorphic mutant, *ct98*, which in contrast to the mutants just mentioned, has meiotic rather than mitotic defects (Table 1, lines 6–7). These results suggest that *tba-2(sb51)* likely interferes with both meiotic and mitotic spindle formation. Because *tba-2(sb51)* enhances mutations that either increase or decrease MEI-1/MEI-2 activity, it likely does not affect microtubule severing *per se*, but may instead affect an element common to both meiotic and mitotic spindles.

***sb51* is a *tba-2* α -tubulin allele:** *sb51* was genetically mapped between two cloned markers, *unc-101* and *unc-59* (MATERIALS AND METHODS). Further SNP mapping (WICKS *et al.* 2001) identified *tba-2* as a likely candidate in the region. Sequencing of the *tba-2* genomic DNA in the *sb51* mutant worms identified a single missense mutation resulting in a Ser168Tyr amino acid substitution (Figure 2). Therefore, *mel-45(sb51)* has been renamed *tbb-2(sb51)*.

Since *tba-2(sb51)* shows dominant spindle defects, we reasoned that it is likely not a *lf* mutation. A deficiency

of the region, *dxDf2*, shows 68% hatching at the nonpermissive temperature (Table 2), eliminating the possibility that *tba-2* is haplo-insufficient. If *tba-2(sb51)* results in a “poison” gene product, the deleterious effects should be blocked by reducing the gene’s expression. Previous RNAi studies revealed redundant roles of the only two α -tubulins that are expressed at significant levels during embryonic development (BAUGH *et al.* 2003; WRIGHT and HUNTER 2003; PHILLIPS *et al.* 2004); we also observed this using gene-specific RNAi (Table 2, lines 1–3). This allowed us to test whether depleting *tba-2* expression (which in itself is not lethal) in *tba-2(sb51)* heterozygous hermaphrodites could rescue the mutant defects in their progeny. Indeed, when we used isotype-specific RNAi to knock down *tba-2* expression in *tba-2(sb51)/+* mutant hermaphrodites, embryonic lethality was efficiently suppressed. In contrast, RNAi to the other α -tubulin, *tba-1*, enhanced the lethality (Table 2, lines 4–7). This strongly suggests that *sb51* represents a neomorphic *tba-2* mutation that acquired a poisonous activity. This activity likely interferes with the function of both α -tubulin isotypes since the *sb51* phenotypes resemble those seen when general microtubule function is compromised by either drugs or mutations (STROME and WOOD 1983; HYMAN and WHITE 1987; WRIGHT and HUNTER 2003; ELLIS *et al.* 2004; PHILLIPS *et al.* 2004).

Intragenic revertants of *tba-2(sb51)*: In an effort to determine whether the viability of *tba-2*(RNAi) reported here and elsewhere (WRIGHT and HUNTER 2003; PHILLIPS *et al.* 2004) approximates a strong *lf* phenotype, we reverted the dominant *ts tba-2(sb51)* lethality to look for *cis*-linked intragenic revertants (MATERIALS AND METHODS). Two mutations tightly linked to *tba-2(sb51)* were isolated. Sequencing confirmed that both represented intragenic revertants: in addition to the parental *sb51* lesion, *sb51 sb116* contains a Glu22Lys mutation and *sb51 sb117* has a Glu69Lys change within the *tba-2* coding region (Figure 2). Both alleles completely reverted *sb51* dominant lethality and are homozygous fertile (Table 2, lines 8–11). *sb51 sb116* was healthier (Table 2, line 9) and was chosen for further analysis.

sb51 sb116 behaves similarly to a chromosomal deficiency that removes the *tba-2* region: both *sb51/sb51 sb116* and *sb51/dxDf2* showed complete sterility at 25°, like *sb51* homozygotes (Table 2, lines 12–14). In addition, both *sb51 sb116* and *dxDf2* showed a slight dominant suppression of *sb51*: unlike the parental mutation *sb51*, which is sterile at all temperatures, both *trans*-heterozygotes were leaky sterile at 15°. The embryos produced by both show 100% lethality (Table 2, lines 13–14). This indicates that the *sb51* phenotype depends on the dosage of the defective product. Although *sb51 sb116* is genetically similar to *dxDf2*, the revertant is likely not a genetic null of *tba-2* because *sb51 sb116/dxDf2* is more severe than *tba-2*(RNAi) (Table 2, lines 2 and 15) and *sb51 sb116* homozygotes have lower viability than *tba-2*(RNAi) animals (Table 2, lines 2 and 9), which,

TBA-1	1	MREVISIHVGOAGVQIGNACWELCYLEHGIQPDGTMPSDQQADGESFTTFFSDTGNGRYV
TBA-2	1	MREVISIHVGOAGVQIGNACWELCYLEHGIQPDGTMPTQSTNEGESFTTFFSDTGSGRYV
		<i>sb116</i> ↪ K
TBA-1	61	PRSI FVDLEPTVVDEIR TGTYK KLFHPEQMI TGKEDAANNYARGHYTVGKELIDTVLDRI
TBA-2	61	PRSI FVDLEPTVVDEIR TGTYK KLFHPEQMI TGKEDAANNYARGHYTVGKELIDTVLDRI
		<i>sb117</i> ↪ K
TBA-1	121	RRLADNCSGLQGGFFV FHS FGGGTGSGFTSLLMERLSVDYGGKSKLEFSIYPAPQVSTAVV
TBA-2	121	RRLADNCSGLQGGFFV FHS FGGGTGSGFTSLLMERLSVDYGGKSKLEFSIYPAPQVSTAVV
		<i>sb51</i> ↪ Y
TBA-1	181	EPYNSILTTHTTLEHSDCAF MVDNEAI YD ICRRNLSVDRPSYTNLNRIISQVSSITASL
TBA-2	181	EPYNSILTTHTTLEHSDCAF MVDNEAI YD ICRRNLDVERPSYTNLNRIISQVSSITASL
		<i>sb27</i> ↪ K
TBA-1	241	RFDGALNVDLNEFQTNLVP YPRIHFPLAA YTPLISADKAYHEALSVNDITNSCFEPANQM
TBA-2	241	RFDGALNVDLNEFQTNLVP YPRIHFPLAA YTPLISA EKAYHEALSVSDITNSCFEPANQM
		<i>sb25</i> ↪ K
TBA-1	301	VKCDPRHGKYMAVCLLYRGD VVPKDVNTAIAAIKTKRTIQFVDWCPTGFKVGINYPPTV
TBA-2	301	VKCDPRHGKYMAVCLLYRGD VVPKDVNTAIAAIKTKRTIQFVDWCPTGFKVGINYPPTV
TBA-1	361	VPGGDLAKVPRAVCMLSNTTAIAEAWSRLDYKFDLMYAKRA FVHWYV GEGMEEGEFTEAR
TBA-2	361	VPGGDLAKVPRAVCMLSNTTAIAEAWSRLDYKFDLMYAKRA FVHWYV GEGMEEGEFTEAR
TBA-1	421	EDLAALEKDYEEVGADS NEGGNEEEGEEY
TBA-2	421	EDLAALEKDYEEVGADS NEGG-EEEGEEY

FIGURE 2.—Alignment of TBA-1 and TBA-2. TBA-1 and TBA-2 sequences were aligned using the Clustal W program (EMBL-European Bioinformatics Institute). Dark shading indicates regions of identity between TBA-1 and TBA-2 sequences. The amino acid sequence change in each TBA-2 allele is indicated.

as we argue below, likely represents the null phenotype. This suggests, in view of the previous results, that *sb51 sb116* may retain some residual *sb51* poisonous activity, which is dosage dependent.

***sb25* and *sb27*, two alleles of *tba-2*, are suppressors of ectopic MEI-1/MEI-2 expression:** In an independent screen, we identified mutations of *tba-2* that affect microtubules in a different manner than does *sb51*. Mutants that show ectopic MEI-1 and MEI-2 expression during mitotic cleavages are defective in mitotic spindle formation (CLARK-MAGUIRE and MAINS 1994a; SRAYKO *et al.* 2000). In a previous screen to identify genes that function in this pathway, we isolated three mutants that rescued the defects caused by ectopic MEI-1/MEI-2 expression (CLANDININ and MAINS 1993). One of them, *sb26*, was found to be a missense allele of the *tbb-2* β -tubulin gene (LU *et al.* 2004). The other two, *sb25* and *sb27*, like *sb26*, lack visible phenotypes of their own. Both semidominantly suppressed the embryonic lethality caused by ectopic MEI-1/MEI-2 expression of *mei-1(ct46gf)* (Table 3, lines 1–7) and *mel-26* (data not shown). In addition, both *sb25* and *sb27* enhanced the hypomorphic mutant *mei-2(ct98)*, which results in reduced meiotic MEI-1/MEI-2 activity (Table 3, lines 8–10) (MAINS *et al.* 1990a; SRAYKO *et al.* 2000). Therefore, both suppressors behave as if they inhibit the general function

of MEI-1/MEI-2 in both meiosis and mitosis. Neither *sb25* nor *sb27* affected the ectopic localization of the MEI-1/MEI-2 complex (Figure 3), suggesting that they likely interfere with MEI-1/MEI-2 activity rather than with its ability to localize to microtubules. All of these properties of *sb25* and *sb27* also resemble *tbb-2(sb26)* (LU *et al.* 2004), suggesting that they likely function at a similar step of the pathway as does *tbb-2(sb26)*.

Both *sb25* and *sb27* map to the right arm of LG I between *unc-101* and *unc-59*. Further SNP mapping (WICKS *et al.* 2001) indicated that the gene(s) harboring these mutations is on a single cosmid in which the α -tubulin gene *tba-2* resides (MATERIALS AND METHODS). Sequencing *tba-2* genomic DNA in *sb25* and *sb27* mutants revealed, respectively, Glu277Lys and Glu194Lys missense mutations in *tba-2* (Figure 2).

Both *tba-2* alleles genetically act as dominant inhibitors of MEI-1/MEI-2 activity, suggesting that they were likely *gf* rather than *lf* alleles of the α -tubulin gene. Consistent with this, removing one copy of *tba-2* with the chromosomal deficiency *dxDf2* did not suppress but instead slightly enhanced *mei-1(ct46gf)* (Table 4, lines 1–2), indicating that suppression did not result from a loss of gene activity. In addition, *sb25* and *sb27* hemizygotes suppressed *mei-1(ct46gf)* slightly less than did their homozygotes (Table 4, lines 3–8). This is again similar

TABLE 2
sb51 is a neomorphic allele of *tba-2*

Maternal genotype	Embryonic hatching (%)	
	15°	25°
<i>tba-1</i> (RNAi)	ND	89
<i>tba-2</i> (RNAi)	ND	77
<i>tba-1</i> (RNAi); <i>tba-2</i> (RNAi)	ND	0
<i>tba-2</i> (<i>sb51</i>)/+	44	6.1
<i>tba-2</i> (<i>sb51</i>)	Sterile	Sterile
<i>tba-2</i> (<i>sb51</i>)/+; <i>tba-1</i> (RNAi)	ND	0
<i>tba-2</i> (<i>sb51</i>)/+; <i>tba-2</i> (RNAi)	ND	59
<i>tba-2</i> (<i>sb51 sb116</i>)/+	98	99
<i>tba-2</i> (<i>sb51 sb116</i>)	45 ^a	51 ^a
<i>tba-2</i> (<i>sb51 sb117</i>)/+	98	98
<i>tba-2</i> (<i>sb51 sb117</i>)	80	27
+ / <i>dxDf2</i>	68	68
<i>tba-2</i> (<i>sb51</i>)/ <i>dxDf2</i>	0	Sterile
<i>tba-2</i> (<i>sb51</i>)/ <i>tba-2</i> (<i>sb51 sb116</i>)	0	Sterile
<i>tba-2</i> (<i>sb51 sb116</i>)/ <i>dxDf2</i>	87 ^b	Sterile

ND, not determined.

^a *N* = 200–500. All others are >500.

^b Corrected for the 32% lethality of *dxDf2*.

to what we found with *tbb-2*(*sb26*), a *gf* allele of *tbb-2* (LU *et al.* 2004).

It is possible that *sb25* and *sb27* result in the general stabilization of microtubules. However, we previously reported that *tbb-2*(*sb26*) caused microtubules to behave as if they are specifically resistant to MEI-1/MEI-2 katanin activity (LU *et al.* 2004). Similar to *tbb-2*(*sb26*), neither *tba-2*(*sb25*) nor *tba-2*(*sb27*) suppressed a *zyg-9* *ts* allele (KEMPHUES *et al.* 1986) that gives rise to less stable microtubules (Table 3, lines 16–18), suggesting that neither *tba-2* allele results in generally more stable microtubules. The possibility that the *tba-2* alleles generally stabilize microtubules was also tested using an *in vivo* cold-induced microtubule-destabilizing assay (HANNAK *et al.* 2002). In this case, we used the double mutant *tba-2*(*sb27*); *tbb-2*(*sb26*), which has a much stronger effect on microtubules than either of the single mutants (see below). When embryos were placed in a cold environment for 5 min, *tba-2*(*sb27*); *tbb-2*(*sb26*) embryos appeared to have similar or fewer numbers of microtubule bundles as compared to wild-type embryos treated in parallel (Figure 4). When *tba-2*(*sb27*); *tbb-2*(*sb26*) and wild-type embryos were placed at 0° for 8 min or longer, all embryos lacked visible microtubule asters. Therefore, *tba-2*(*sb25*) and *tba-2*(*sb27*) likely result in microtubules specifically resistant to MEI-1/MEI-2 activity without causing obvious effects on general microtubule dynamics.

Microtubules resistant to MEI-1/MEI-2 activity cause meiotic defects: Microtubules showing complete resistance to MEI-1/MEI-2 activity should result in meiotic failure characteristic of *mei-1* or *mei-2* null alleles, yet the *tbb-2* and *tba-2* alleles selected as suppressors of ectopic MEI-1/MEI-2 activity have no apparent phenotype

TABLE 3
Genetics of *tba-2*(*sb25*) and *tba-2*(*sb27*)

Maternal genotype	Embryonic hatching (%)		
	15°	20°	25°
<i>mei-1</i> (<i>ct46</i>)	23	1.5	0
<i>tba-2</i> (<i>sb25</i>)	96	ND	100
<i>mei-1</i> (<i>ct46</i>) <i>tba-2</i> (<i>sb25</i>)/ <i>mei-1</i> (<i>ct46</i>) +	ND	12	0
<i>mei-1</i> (<i>ct46</i>) <i>tba-2</i> (<i>sb25</i>)	75	57	15
<i>tba-2</i> (<i>sb27</i>)	97	ND	98
<i>mei-1</i> (<i>ct46</i>) <i>tba-2</i> (<i>sb27</i>)/ <i>mei-1</i> (<i>ct46</i>) +	ND	15	0
<i>mei-1</i> (<i>ct46</i>) <i>tba-2</i> (<i>sb27</i>)	66	55	12
<i>mei-2</i> (<i>ct98</i>)	96	ND	74
<i>mei-2</i> (<i>ct98</i>) <i>tba-2</i> (<i>sb25</i>)	98	ND	43
<i>mei-2</i> (<i>ct98</i>) <i>tba-2</i> (<i>sb27</i>)	10	ND	0.9
<i>tbb-2</i> (<i>sb26</i>)	98	ND	97
<i>tba-2</i> (<i>sb27</i>); <i>tbb-2</i> (<i>sb26</i>)	88 (2) ^a	ND	44 (11) ^a
<i>tba-2</i> (<i>sb25</i>); <i>tbb-2</i> (<i>sb26</i>)	94	ND	99
<i>mei-1</i> (<i>ct46</i>) <i>tba-2</i> (<i>sb25</i>); <i>tbb-2</i> (<i>sb26</i>)	ND	99	91
<i>mei-1</i> (<i>ct46</i>); <i>tbb-2</i> (<i>sb26</i>)	96 ^b	92 ^b	67 ^b
<i>zyg-9</i> (<i>b244</i>)	ND	97	0
<i>tba-2</i> (<i>sb25</i>); <i>zyg-9</i> (<i>b244</i>)	ND	98	0
<i>tba-2</i> (<i>sb27</i>); <i>zyg-9</i> (<i>b244</i>)	ND	93	0

ND, not determined.

^a Percentage of males among survivors. In wild type, only 0.2% of self-progeny are male (HODGKIN and BRENNER 1977).

^b Data taken from LU *et al.* (2004).

on their own. Therefore, each likely renders only partial resistance. We speculated that the effect of combining an α -tubulin and the β -tubulin suppressor mutation would be additive, perhaps resulting in meiotic defects similar to those of *mei-1/mei-2 lf* mutants. Indeed, *tba-2*(*sb27*); *tbb-2*(*sb26*) double-mutant adults are healthy with normal brood size but displayed only 44% hatching at 25° (Table 3, line 12). As shown in Figure 5, a *tba-2*(*sb27*); *tbb-2*(*sb26*) embryo showed normal pronuclear fusion and normal first mitotic cleavage. However, abnormally large polar bodies often (4/9) formed at the anterior, indicative of meiotic defects (Figure 5, D–F), and such embryos would likely die due to the resulting aneuploidy. Among the survivors at 25°, there was also a high incident of male (Him) phenotype (Table 3, line 12), which is also indicative of meiotic failure leading to nondisjunction that gives rise to XO males (HODGKIN and BRENNER 1977). The polar body and Him phenotypes are typical of *mei-1* and *mei-2* hypomorphs, which have minor meiotic spindle defects (MAINS *et al.* 1990a). Indeed, meiotic spindles of *tba-2*(*sb27*); *tbb-2*(*sb26*) embryos show abnormal morphologies comparable to meiotic spindles from the *mei-2* hypomorphic allele *ct98* (Figure 6, A–C). However, the meiotic spindle defects are not as severe as those seen in the *mei-1*(*ct46ct101*) null mutant, which has a cloud of microtubules that does not coalesce into a spindle (Figure 6D). Animals doubly mutant for *tbb-2*(*sb26*) and the other *tba-2* muta-

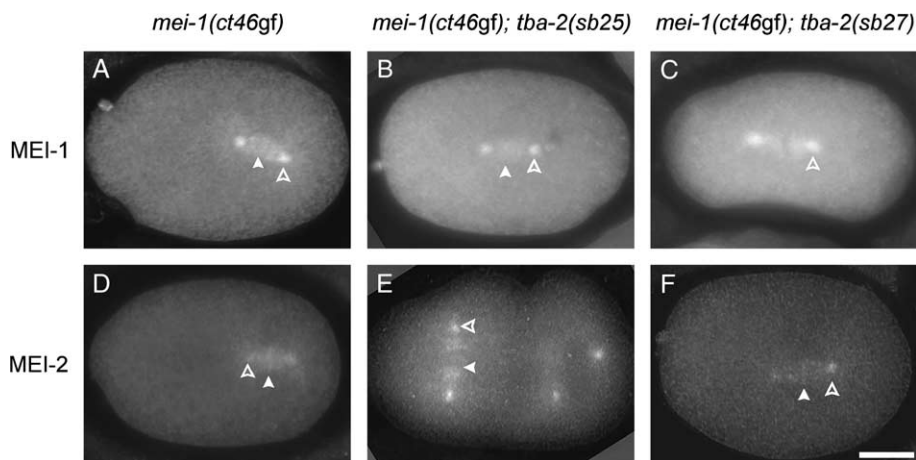


FIGURE 3.—Mislocalization of MEI-1 and MEI-2 to mitotic centrosomes and chromosomes in *mei-1(ct46); tba-2(sb25)* and *mei-1(ct46); tba-2(sb27)* double-mutant embryos. Indirect immunofluorescence images of anti-MEI-1 staining show ectopic MEI-1 expression in (A) *mei-1(ct46gf)*, (B) *mei-1(ct46gf); tba-2(sb25)*, and (C) *mei-1(ct46gf); tba-2(sb27)*. Similar results were seen with anti-MEI-2 staining in (D) *mei-1(ct46gf)*, (E) *mei-1(ct46gf); tba-2(sb25)*, and (F) *mei-1(ct46gf); tba-2(sb27)*. Both MEI-1 and MEI-2 localize to mitotic spindle microtubules, centrosomes (open arrowheads), and chromosomes (open arrowheads). The photographs were digitally deconvolved. Bar, 10 μ m.

tions, *sb25*, did not have obvious meiotic defects like those seen in *tba-2(sb27); tbb-2(sb26)* (Table 3, line 13). Nevertheless, they also behaved as if their microtubules were more resistant to katanin activity than the single mutants since the *mei-1(ct46gf)* lethality was almost completely suppressed, giving rise to 91% hatching at the restrictive temperature (Table 3, line 14), as compared to 15% hatching for *mei-1(ct46) tba-2(sb25)* and 67% for *mei-1(ct46); tbb-2(sb26)* (Table 3, lines 4 and 15).

TBA-2 and TBA-1 interact differently with MEI-1/MEI-2: We previously reported that *mei-1/mei-2* showed different genetic interactions with null alleles of the two redundant β -tubulin isotypes, *tbb-1* and *tbb-2*, suggesting that microtubules containing the TBB-2 isotype are preferred by the MEI-1/MEI-2 microtubule-severing complex (LU *et al.* 2004). We asked whether the TBA-1 and TBA-2 isotypes are also differentially required for the activity of MEI-1/MEI-2. Wild-type meiotic embryos contain excess MEI-1/MEI-2 activity (CLANDININ and MAINS 1993), which can mask subtle functional differences among tubulin isotypes. Therefore, we used the partial *lf* allele *mei-2(ct98)* to lower (but not eliminate) meiotic MEI-1/MEI-2 activity and examined the effects of depleting either TBA-1 or TBA-2 by gene-specific RNAi.

TABLE 4

sb25 and *sb27* are both gain-of-function suppressors of *mei-1(ct46)*

Maternal genotype	Embryonic hatching at 20° (%)
<i>mei-1(ct46)/+</i>	27
<i>mei-1(ct46) tba-2(+)/+ dxDf2</i>	12 ^a
<i>mei-1(ct46) tba-2(sb25)/+ +</i>	44
<i>mei-1(ct46) tba-2(sb25)/+ tba-2(sb25)</i>	90
<i>mei-1(ct46) tba-2(sb25)/+ dxDf2</i>	78 ^a
<i>mei-1(ct46) tba-2(sb27)/+ +</i>	42
<i>mei-1(ct46) tba-2(sb27)/+ tba-2(sb27)</i>	78
<i>mei-1(ct46) tba-2(sb27)/+ dxDf2</i>	70 ^a

^a Corrected for the 32% lethality of *dxDf2*.

Depleting TBA-2 in *mei-2(ct98)* strongly enhanced its meiotic lethality, while depletion of TBA-1 had only a small effect (Table 5, lines 1–5, and Table 6). This suggests that the activity of MEI-1/MEI-2 prefers microtubules containing the TBA-2 isotype. Therefore, MEI-1/MEI-2 appears to interact differentially with superficially very similar α -tubulin isotypes.

It is formally possible that the differential effects that we observed above resulted from the unequal efficiency of *tba-1* and *tbb-2* RNAi. The high sequence similarity

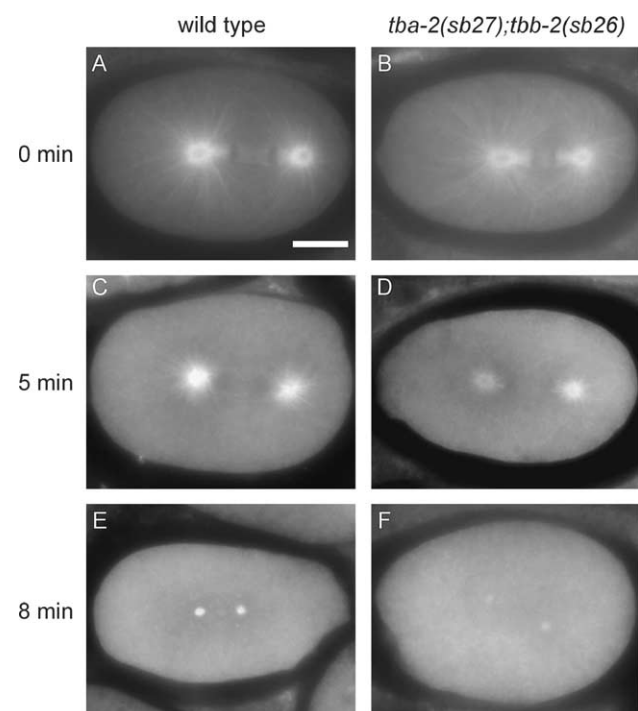


FIGURE 4.—*tba-2(sb27); tbb-2(sb26)* and wild-type microtubules behave similarly in a cold environment. Representative one-cell embryos of wild-type (A, C, and E) and *tba-2(sb27); tbb-2(sb26)* (B, D, and F) embryos ($n > 20$ for both genotypes) were placed on ice for 0 (A and B), 5 (C and D), and 8 (E and F) min, fixed, and stained with anti- α -tubulin antibody to visualize spindle microtubule structure. Bar, 10 μ m.

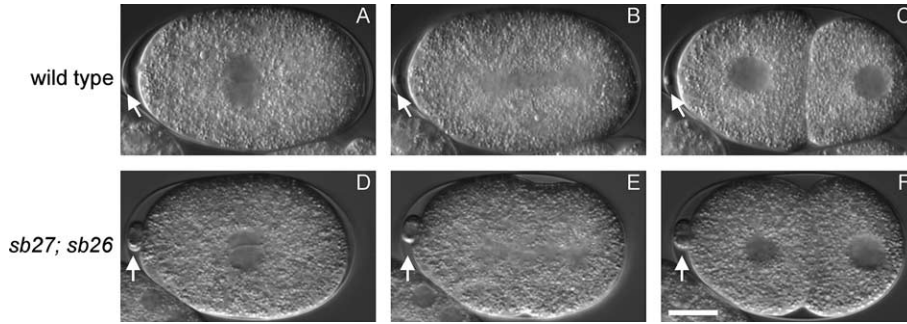


FIGURE 5.—Meiotic phenotype of the *tba-2(sb25); tbb-2(sb26)* double mutant. Shown are Nomarski images of the first cell division of a wild-type embryo (A–C) and of a *tba-2(sb25); tbb-2(sb26)* embryo (D–F) at 25°. In *tba-2(sb25); tbb-2(sb26)* embryos, female and male pronuclei migrate normally to the center of the embryo and rotate 90° (D); then the first mitotic spindle is aligned longitudinally (E), and the cell divides asymmetrically into a larger anterior daughter and a smaller posterior

daughter (F). All of these features resemble those of wild type (A–C). However, *tba-2(sb25); tbb-2(sb26)* embryos often have enlarged polar bodies (open arrow; compare D–F to A–C), indicating meiotic spindle defects. Bar, 10 μ m.

between these two genes makes generation of isotype-specific antibodies impractical for examining the effects of RNAi on gene expression. We reasoned that if the different effects seen in the *mei-2(ct98)* background reflect differences of RNAi-mediated depletion of gene expression, then these effects should vary when concentrations of the double-stranded RNA change. However, as shown in Table 6, the differential effects of *tba-1* and *tba-2* RNAi remained consistent when RNA concentrations changed over a 10-fold range: the enhancement of *mei-2(ct98)* lethality by *tba-2*(RNAi) was dose dependent, while little or no effect was seen for *tba-1* RNAi even at the highest concentration. The observation that the double RNAi showed almost complete lethality at a lower dose (0.5 mg/ml) indicates that each single RNAi works efficiently at this lower concentration. Therefore, when the highest concentration (2.5 mg/ml) was used in the RNAi experiments, *tba-1* and *tba-2* RNAi pheno-

types likely closely approximated null phenotypes, supporting our suggestion for the TBA-2 isotype preference by MEI-1/MEI-2 katanin.

The viability of *tba-2*(RNAi) and *tba-2(sb51sb116)* indicates that the preference of MEI-1/MEI-2 for TBA-2 is not absolute (otherwise they would mimic the *mei-1(null)* phenotype), and so microtubules containing only TBA-1 must be a usable substrate when MEI-1/MEI-2 is not limiting. This was also true for microtubules containing only TBB-1, which can serve as a MEI-1/MEI-2 substrate when the preferred β -isotype, TBB-2, is eliminated by either mutation or RNAi (LU *et al.* 2004) in an otherwise wild-type background. We next asked if removal of both preferred isotypes, TBA-2 (by RNAi) and TBB-2 (using a deletion mutant), resulted in microtubules that are resistant to wild-type levels of MEI-1/MEI-2 activity. However, in the absence of both of the two preferred

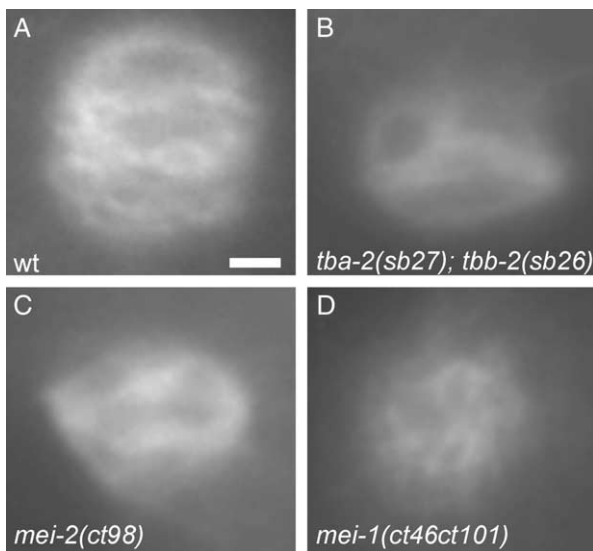


FIGURE 6.—Meiotic spindle defects of *tba-2(sb27); tbb-2(sb26)* mutant embryos. Anti- α -tubulin staining of metaphase or early anaphase meiotic spindles of (A) wild-type, (B) *tba-2(sb27); tbb-2(sb26)*, (C) *mei-2(ct98)*, and (D) *mei-1(ct46ct101)* embryos are shown to reveal morphological defects of the mutant spindles. Bar, 2 μ m.

TABLE 5
MEI-1/MEI-2 prefers TBA-2

Maternal genotype	Embryonic hatching at 25° (%)
<i>tba-1</i> (RNAi)	89 ^a
<i>tba-2</i> (RNAi)	77 ^a
<i>mei-2(ct98)</i>	71
<i>mei-2(ct98); tba-1</i> (RNAi)	55
<i>mei-2(ct98); tba-2</i> (RNAi)	8
<i>tbb-2(gk129)</i>	65
<i>tba-2</i> (RNAi); <i>tbb-2(gk129)</i>	63
<i>tbb-2(sb26)</i>	97
<i>tba-1</i> (RNAi); <i>tbb-2(sb26)</i>	87
<i>tba-2</i> (RNAi); <i>tbb-2(sb26)</i>	65
<i>tbb-1(gk207)</i>	94
<i>tba-1</i> (RNAi); <i>tbb-1(gk207)</i>	92
<i>tba-2</i> (RNAi); <i>tbb-1(gk207)</i>	81
<i>tba-1</i> (RNAi); <i>tbb-2(gk129)</i>	60

^a Numbers taken from Table 2. Double-stranded RNAs were used at 0.5 mg/ml for *tba-1* and *tba-2* throughout this table. These concentrations of double-stranded RNA resulted in complete lethality for the *tba-1* and *tba-2* double RNAi (Table 2), indicating that each must eliminate a substantial amount of its respective product.

TABLE 6
tba-1 and *tba-2* RNAi effects at different concentrations

dsRNA concentration (mg/ml)	Embryonic hatching at 25° (%)				
	<i>tba-1</i> RNAi		<i>tba-2</i> RNAi		<i>tba-1</i> and <i>tba-2</i> RNAi:
	N2	<i>mei-2(ct98)</i>	N2	<i>mei-2(ct98)</i>	N2
2.5	91	55	89	0.4	0
0.5	89	55	77	8	0
0.25	96	69	84	17	0.6
0.025	96	66	91	69	48

tubulin isotypes, TBB-2 and TBA-2, embryos developed relatively normally, without showing increased lethality relative to the single depletions or any obvious meiotic spindle defects (Table 5, lines 2, 6–7). This suggests that the pair is not absolutely required when MEI-1/MEI-2 katanin is not limiting. We also eliminated the preferred *tba-2* isotype in the presence of the resistant *tbb-2(sb26)* allele, but again found at best a modest effect (Table 5, lines 8–10).

To determine if there is a requirement for one particular type of α/β heterodimer for viability, we used *tbb-1* and *tba-2* deletion alleles in combination with *tba-1*(RNAi) and *tba-2*(RNAi) to deplete the other pairwise α - and β -tubulin combinations. As shown in Table 5, we found that removing any combinations of α - and β -isotypes did not decrease hatching rates and resulted in relatively normal development. No obvious meiotic defects were observed (Table 5, lines 12–14). Therefore, the presence of one α - and one β -isotype, regardless of which of the two, suffices for development.

DISCUSSION

C. elegans female meiosis and the subsequent first mitosis require very distinctive types of spindle organization despite the fact that both occur in a common cytoplasm within a short period of time (ALBERTSON 1984; KEMPHUES *et al.* 1986). Therefore, the microtubule cytoskeleton must be precisely regulated during these divisions. While the MEI-1/MEI-2 katanin microtubule-severing activity is essential for meiotic spindle organization, its ectopic presence in subsequent mitotic divisions results in displacement of the mitotic spindle and shorter astral microtubules (CLARK-MAGUIRE and MAINS 1994a; SRAYKO *et al.* 2000). Factors like MEI-1 and MEI-2 must adjust spindle microtubule dynamics or function to achieve different morphological and functional requirements in meiosis and mitosis. Microtubule-stabilizing factors, such as ZYG-9, also play a role in the formation of both spindles, and ZYG-9 activity seems to be counterbalanced by *mei-1* and *mei-2* in meiosis (MATTHEWS *et al.* 1998; BELLANGER and GONCZY 2003; SRAYKO *et al.* 2003).

A *tba-2* mutation destabilizes microtubules: Tubulin mutations that affect the general dynamic properties of microtubules are expected to show spindle defects in both meiosis and mitosis. Here we have shown that the *tba-2* α -tubulin mutation *sb51* results in dominant, *ts* maternal-effect lethality due to defective spindle formation in both meiosis and mitosis. *tba-2(sb51)* mitotic defects resemble those of embryos treated with microtubule-depolymerizing drugs (STROME and WOOD 1983; HYMAN and WHITE 1987), suggesting that *sb51* inhibits microtubule assembly and/or stability. Mutations that result in ectopic MEI-1/MEI-2 activity during mitosis also result in similar phenotypes, and indeed, such mutations enhanced *tba-2(sb51)* lethality (Table 2). However, the *tba-2(sb51)* mitotic spindle defects do not depend on MEI-1/MEI-2 activity since there is no ectopic MEI-1/MEI-2 present in mitosis in *tba-2(sb51)* embryos (data not shown) and *sb51* dominant lethality is not affected by *tbb-2(sb26)*, which results in microtubules less sensitive to MEI-1/MEI-2 activity (data not shown). In addition, *tba-2(sb51)* homozygotes are sterile due to insufficient germline mitotic proliferation (data not shown), a process also independent of MEI-1 and MEI-2. The enhancement of embryonic lethality between *tba-2(sb51)* and *mei-1* pathway mutants likely reflects synergism between mutations that independently weaken the mitotic spindle. *tba-2(sb51)* also enhances a *mei-2* hypomorphic mutation that limits the normal meiotic microtubule-severing activity of MEI-1/MEI-2. In this background, microtubules would be expected to be more stable due to decreased microtubule severing, indicating that the *mei-2/tba-2* (*sb51*) genetic interaction likely reflects synergism between spindles that are defective in different ways.

The simplest explanation of the *tba-2(sb51)* dominant phenotype is that it acts as a neomorphic poison that inhibits microtubule assembly and/or function. Since RNAi (Table 2) (WRIGHT and HUNTER 2003; PHILLIPS *et al.* 2004) and intragenic *lf* revertants (Table 2) demonstrate that *tba-2* is nonessential (due to redundancy with *tba-1*), *sb51* likely acts by inhibiting both *tba-1* and *tba-2* function. *tba-2(sb51)* might form heterodimers with the β -tubulin isotypes that cannot either assemble or result in unstable microtubules. Consistent with the neomor-

phic poisonous effect of *tba-2(sb51)*, *tba-2*(RNAi) rescued *sb51* dominant lethality while *tba-1*(RNAi) enhanced it. The *sb51* lesion Ser168Tyr is located at the edge of the T5 loop that makes contact with the ribose of GTP (LÖWE *et al.* 2001). Therefore, TBA-2(*sb51*) likely has an altered conformation in the GTP-bound form, which may dominantly disrupt microtubule dynamics when incorporated into tubulin heterodimers or microtubules.

Most of the poisonous effect of *tba-2(sb51)* was suppressed by the intragenic revertant *sb51 sb116*. *sb51 sb116* has a second-site Glu22Lys mutation in TBA-2 (Figure 2), a region suggested to affect interaction with the phosphates of the α -tubulin bound nonexchangeable GTP (NOGALES *et al.* 1998). *sb51 sb116* most likely results in a subunit that is unstable or that cannot interact with β -tubulin, and so it would also no longer antagonize TBA-1. A TBA-2-specific antibody would test this hypothesis. However, due to the extremely high amino acid sequence conservation between TBA-1 and TBA-2, which are 98.5% identical, raising an isotype-specific antibody to follow the fate of the mutant protein is not feasible. *sb51 sb117* has a second-site Glu69Lys mutation that likely also affects TBA-2 interactions with phosphates of GTP and so may exert an effect similar, but weaker, to that seen for *sb51 sb116*.

α - and β -tubulin mutations with phenotypes similar to *tba-2(sb51)* have also been identified in *C. elegans* by other groups. These mutations are thought to exert their effects through different mechanisms. TBB-2(*or362*) is a Gly-to-Glu mutation at position 141 within one of the GTP-binding domains, and the mutant protein is expressed at a very low level. However, this conditionally semidominant mutation, like *tba-2(sb51)/+*, poisons spindle microtubules and causes strong spindle defects (ELLIS *et al.* 2004). TBB-2(*qt1*) has a Glu-to-Lys change at position 198 and appears to increase microtubule stability when incorporated (WRIGHT and HUNTER 2003). TBB-2(*t1623*) has a Val-to-Met change at position 313 (WRIGHT and HUNTER 2003) and has decreased TBB-2 levels that are still sufficient for incorporation into the spindle. The α -tubulin mutant TBA-1(*or346*) has a Ser-to-Phe change at position 379 (PHILLIPS *et al.* 2004) and behaves as a conditionally semidominant poison mutation. Both TBB-2(*t1623*) and TBA-1(*or346*) likely affect spindle formation by disrupting microtubule dynamics or its interactions with MAPs.

Mutations in *tba-2* increase microtubule resistance to MEI-1/MEI-2 activity: MEI-1/MEI-2 microtubule severing must require specific interactions with tubulins, and we have identified mutant tubulins that appear to interfere with this interaction. We previously demonstrated that the β -tubulin mutation *tbb-2(sb26)* partially inhibited MEI-1/MEI-2 activity, likely at the level of severing since localization to microtubules was not affected. This allele is a point mutation in the carboxyl terminus of the TBB-2 β -tubulin (LU *et al.* 2004). In contrast to the rest of the protein, the carboxyl termini

of tubulins generally show low sequence conservation and are the most obvious distinguishing features among isotypes (although this is not true for *tba-1* and *tba-2*; Figure 2). This region was previously shown to be required for *in vitro* katanin severing (MCNALLY and VALE 1993). Here we show that the *sb25* and *sb27* mutations of *tba-2* similarly result in partial resistance to MEI-1/MEI-2 function, again without affecting MEI-1/MEI-2 localization to microtubules (Figure 3). Unlike *tbb-2(sb26)*, their lesions are well outside the carboxyl terminus, implicating other regions of the protein for MEI-1/MEI-2 interactions. Interestingly, similar to the amino acid substitution in TBB-2(*sb26*), both *sb25* and *sb27* resulted in Glu-to-Lys changes (at residues 277 and 194, respectively; Figure 2), decreasing the acidity of the protein. Although the two mutations are not close to one another in the protein sequence, they both fall into a region in the 3D structure where strong lateral contacts between protofilaments are made (NOGALES *et al.* 1998). Thus, the *tba-2* mutations could act by increasing the general stability of the microtubules rather than by altering specific interactions with MEI-1/MEI-2. However, this is not likely since neither *tba-2(sb25)* nor *tba-2(sb27)* genetically interacted with *zyg-9(ts)* (Table 3) or *zyg-9*(RNAi) (data not shown), which encodes a MAP that stabilizes microtubules (MATTHEWS *et al.* 1998). In addition, this model might predict that microtubules containing these *tba-2* mutations would be more cold stable (HANNAK *et al.* 2002). However, the cold stability of microtubules in early *tba-2(sb27)*; *tbb-2(sb26)* embryos was not altered (Figure 4), suggesting that these mutations specifically affect the interactions between katanin and microtubules. Furthermore, *tba-2(sb27)*; *tbb-2(sb26)* embryos displayed defects only in meiosis where MEI-1/MEI-2 activity is normally present (Figures 5 and 6). Therefore, these genetic studies strongly suggest that the three tubulin mutations, *sb25*, *sb26*, and *sb27*, specifically disrupt katanin-microtubule interactions required for severing rather than general microtubule stability, hence rendering microtubules less sensitive to katanin activity.

Microtubules containing any one of the tubulin mutations are not completely resistance to MEI-1/MEI-2 activity since none of the mutants alone showed defects in meiosis, where katanin activity is essential (MAINS *et al.* 1990a; SRAYKO *et al.* 2000). Meiotic phenotypes were seen only when *tba-2* and *tbb-2* alleles were combined (Table 3 and Figure 5). The three mutations differ individually in the degree of their resulting resistance to MEI-1/MEI-2 activity. *sb27* showed the strongest enhancement of *mei-2(lf)*, implying that it confers on microtubules the strongest resistance among the three. However, *sb27* is not the best suppressor of *mei-1(ct46gf)* (Table 3). This is likely due to the *mei-1(ct46gf)* mutation, which in addition to resulting in mitotic persistence of the mutant product, reduces MEI-1 activity during meiosis to some extent (but not to lethal levels;

data not shown). Hence, strong suppression of the ectopic mitotic activity of *mei-1(ct46gf)* by *sb27* would be masked by the corresponding increased lethality resulting from its enhancement of the *mei-1(ct46gf)* meiotic defects (data not shown).

Redundant tubulin isotypes differ in their interactions with MEI-1/MEI-2: Microarray data indicate that the early *C. elegans* embryo expresses a pair of α - and a pair of β -tubulin isotypes (BAUGH *et al.* 2003). In both cases, these are the only isotypes expressed at significant levels, and members of each pair are expressed at similar levels. Using RNAi and null mutants, we and others have demonstrated that members of each pair are redundant for viability (LU *et al.* 2004; PHILLIPS *et al.* 2004). WRIGHT and HUNTER (2003) showed previously that simultaneous depletion TBA-2 and TBB-2 expression resulted in high (although not complete) lethality while we observed a lower level of lethality (Table 5). However, this difference was mainly due to the high embryonic lethality (90%) that the authors observed with the strains containing the *tbb-2* deletion allele. However, we found both *tbb-2* deletion alleles were much healthier after outcrossing (LU *et al.* 2004), and these outcrossed strains were used in the work reported here.

Using the sensitized genetic background of *mei-2(ct98)*, which lowers but does not eliminate MEI-1/MEI-2 activity in meiosis, we showed that one member of each isotypic pair, TBB-2 and TBA-2, is preferred for katanin activity (Tables 5 and 6 and LU *et al.* 2004). Simultaneous elimination of *tba-2* and *tbb-2* resulted 63% hatching (Table 5) with no obvious meiotic defects. Thus, we have shown that the worm encodes both α - and β -tubulin isotypes that are specialized for interactions with MEI-1/MEI-2 katanin activity, although those specializations are not absolute. Thus although tubulin isotypes often appear superficially similar in function, but they can indeed have subtle distinctions that are likely advantageous in nature.

We thank B. Bowerman, C. Hunter, G. Ellis, and A. Wright for communicating unpublished results, J. Phillips for sharing reagents, and F. McNally and members of the Mains, McGhee, Brook, and Gaudet labs for helpful discussion. We thank the *C. elegans* Reverse Genetics Core Facility at the University of British Columbia (funded by the Canadian Institute for Health Research, Genome Canada and Genome British Columbia) for *tbb-2* and *tbb-1* deletion strains, Y. Kohara for cDNA clones, and T. Stiernagle at the *Caenorhabditis elegans* Genetics Center (funded by the National Institutes of Health, Center for Research Resources) for providing several strains used in this study. This work was supported by grants from the Canadian Institute of Health Research and the Alberta Heritage Foundation for Medical Research to P.E.M. and by a Canadian Institute of Health Research graduate student voucher to C.L.

LITERATURE CITED

- ALBERTSON, D. G., 1984 Formation of the first cleavage spindle in nematode embryos. *Dev. Biol.* **101**: 61–72.
- ANDERS, K. R., and D. BOTSTEIN, 2001 Dominant-lethal alpha-tubulin mutants defective in microtubule depolymerization in yeast. *Mol. Biol. Cell* **12**: 3973–3986.
- BAUGH, L. R., A. A. HILL, D. K. SLONIM, E. L. BROWN and C. P. HUNTER, 2003 Composition and dynamics of the *Caenorhabditis elegans* early embryonic transcriptome. *Development* **130**: 889–900.
- BELLANGER, J. M., and P. GONCZY, 2003 TAC-1 and ZYG-9 form a complex that promotes microtubule assembly in *C. elegans* embryos. *Curt. Biol.* **13**: 1488–1498.
- BODE, C. J., M. L. GUPTA, K. A. SUPRENTANT and R. H. HIMES, 2003 The two alpha-tubulin isotypes in budding yeast have opposing effects on microtubule dynamics *in vitro*. *EMBO Rep.* **4**: 94–99.
- BRENNER, S., 1974 The genetics of *Caenorhabditis elegans*. *Genetics* **77**: 71–94.
- CLANDININ, T. R., and P. E. MAINS, 1993 Genetic studies of *mei-1* gene activity during the transition from meiosis to mitosis in *Caenorhabditis elegans*. *Genetics* **134**: 199–210.
- CLARK-MAGUIRE, S., and P. E. MAINS, 1994a Localization of the *mei-1* gene product of *Caenorhabditis elegans*, a meiotic-specific spindle component. *J. Cell Biol.* **126**: 199–209.
- DAVIS, A., C. R. SAGE, C. A. DOUGHERTY and K. W. FARRELL, 1994 Microtubule dynamics modulated by guanosine triphosphate hydrolysis activity of beta-tubulin. *Science* **264**: 839–842.
- DERRY, W. B., L. WILSON, I. A. KHAN, R. F. LUDUENA and M. A. JORDAN, 1997 Taxol differentially modulates the dynamics of microtubules assembled from unfractionated and purified beta-tubulin isotypes. *Biochemistry* **36**: 3554–3562.
- DESAI, A., and T. J. MITCHISON, 1997 Microtubule polymerization dynamics. *Annu. Rev. Cell Dev. Biol.* **13**: 83–117.
- DOUGHERTY, C. A., C. R. SAGE, A. DAVIS and K. W. FARRELL, 2001 Mutation in the beta-tubulin signature motif suppresses microtubule GTPase activity and dynamics, and slows mitosis. *Biochemistry* **40**: 15725–15732.
- DOW, M. R., and P. E. MAINS, 1998 Genetic and molecular characterization of the *Caenorhabditis elegans* gene, *mel-26*, a postmeiotic negative regulator of *mei-1*, a meiotic-specific spindle component. *Genetics* **150**: 119–128.
- EDGAR, L. G., and J. D. MCGHEE, 1986 Embryonic expression of a gut-specific esterase in *Caenorhabditis elegans*. *Dev. Biol.* **114**: 109–118.
- ELLIS, G. C., J. B. PHILLIPS, S. O'ROURKE, R. LYCZAK and B. BOWERMAN, 2004 Maternally expressed and partially redundant beta-tubulins in *Caenorhabditis elegans* are autoregulated. *J. Cell Sci.* **117**: 457–464.
- FRASER, A. G., R. S. KAMATH, P. ZIPPERLEN, M. MARTINEZ-CAMPOS, M. SOHRMANN *et al.*, 2000 Functional genomic analysis of *C. elegans* chromosome I by systematic RNA interference. *Nature* **408**: 325–330.
- FUKUSHIGE, T., Z. K. SIDDIQUI, M. CHOU, J. G. CULOTTI, C. B. GOGONEA *et al.*, 1999 MEC-12, an alpha-tubulin required for touch sensitivity in *C. elegans*. *J. Cell Sci.* **112** (Pt. 3): 395–403.
- FURUKAWA, M., Y. J. HE, C. BORCHERS and Y. XIONG, 2003 Targeting of protein ubiquitination by BTB-Cullin 3-Roc1 ubiquitin ligases. *Nat. Cell Biol.* **5**: 1001–1007.
- HANNAK, E., K. OEGEMA, M. KIRKHAM, P. GONCZY, B. HABERMANN *et al.*, 2002 The kinetically dominant assembly pathway for centrosomal asters in *Caenorhabditis elegans* is gamma-tubulin dependent. *J. Cell Biol.* **157**: 591–602.
- HODGKIN, J. A., and S. BRENNER, 1977 Mutations causing transformation of sexual phenotype in the nematode *Caenorhabditis elegans*. *Genetics* **86**: 275–287.
- HOYLE, H. D., and E. C. RAFF, 1990 Two *Drosophila* beta tubulin isoforms are not functionally equivalent. *J. Cell Biol.* **111**: 1009–1026.
- HUNTER, A. W., M. CAPLOW, D. L. COY, W. O. HANCOCK, S. DIEZ *et al.*, 2003 The kinesin-related protein MCAK is a microtubule depolymerase that forms an ATP-hydrolyzing complex at microtubule ends. *Mol. Cell* **11**: 445–457.
- HYMAN, A. A., and J. G. WHITE, 1987 Determination of cell division axes in the early embryogenesis of *Caenorhabditis elegans*. *J. Cell Biol.* **105**: 2123–2135.
- KEMPHUES, K. J., N. WOLF, W. B. WOOD and D. HIRSH, 1986 Two loci required for cytoplasmic organization in early embryos of *Caenorhabditis elegans*. *Dev. Biol.* **113**: 449–460.
- KURZ, T., L. PINTARD, J. H. WILLIS, D. R. HAMILL, P. GONCZY *et*

- al., 2002 Cytoskeletal regulation by the Nedd8 ubiquitin-like protein modification pathway. *Science* **295**: 1294–1298.
- LÖWE, J., H. LI, K. H. DOWNING and E. NOGALES, 2001 Refined structure of alpha beta-tubulin at 3.5 Å resolution. *J. Mol. Biol.* **313**: 1045–1057.
- LU, C., M. SRAYKO and P. E. MAINS, 2004 The *Caenorhabditis elegans* microtubule-severing complex MEI-1/MEI-2 katanin interacts differently with two superficially redundant {beta}-tubulin isoforms. *Mol. Biol. Cell* **15**: 142–150.
- LUDUENA, R. F., 1998 Multiple forms of tubulin: different gene products and covalent modifications. *Int. Rev. Cytol.* **178**: 207–275.
- MAINS, P. E., K. J. KEMPHUES, S. A. SPRUNGER, I. A. SULSTON and W. B. WOOD, 1990a Mutations affecting the meiotic and mitotic divisions of the early *Caenorhabditis elegans* embryo. *Genetics* **126**: 593–605.
- MAINS, P. E., I. A. SULSTON and W. B. WOOD, 1990b Dominant maternal-effect mutations causing embryonic lethality in *Caenorhabditis elegans*. *Genetics* **125**: 351–369.
- MATTHEWS, L. R., P. CARTER, D. THIERRY-MIEG and K. KEMPHUES, 1998 ZYG-9, a *Caenorhabditis elegans* protein required for microtubule organization and function, is a component of meiotic and mitotic spindle poles. *J. Cell Biol.* **141**: 1159–1168.
- M McNALLY, F. J., and R. D. VALE, 1993 Identification of katanin, an ATPase that severs and disassembles stable microtubules. *Cell* **75**: 419–429.
- MITCHISON, T. J., 1989 Polewards microtubule flux in the mitotic spindle: evidence from photoactivation of fluorescence. *J. Cell Biol.* **109**: 637–652.
- MITCHISON, T., and M. KIRSCHNER, 1984 Dynamic instability of microtubule growth. *Nature* **312**: 237–242.
- MITENKO, N. L., J. R. EISNER, J. R. SWISTON and P. E. MAINS, 1997 A limited number of *Caenorhabditis elegans* genes are readily mutable to dominant, temperature-sensitive maternal-effect embryonic lethality. *Genetics* **147**: 1665–1674.
- NOGALES, E., S. G. WOLF and K. H. DOWNING, 1998 Structure of the alpha beta tubulin dimer by electron crystallography. *Nature* **391**: 199–203.
- PANDA, D., H. P. MILLER, A. BANERJEE, R. F. LUDUENA and L. WILSON, 1994 Microtubule dynamics *in vitro* are regulated by the tubulin isotype composition. *Proc. Natl. Acad. Sci. USA* **91**: 11358–11362.
- PHILLIPS, J. B., R. LYCZAK, G. C. ELLIS and B. BOWERMAN, 2004 Roles for two partially redundant alpha-tubulins during mitosis in early *Caenorhabditis elegans* embryos. *Cell Motil. Cytoskeleton* **58**: 112–126.
- PINTARD, L., J. H. WILLIS, A. WILLEMS, J. L. JOHNSON, M. SRAYKO *et al.*, 2003 The BTB protein MEL-26 is a substrate-specific adaptor of the CUL-3 ubiquitin-ligase. *Nature* **425**: 311–316.
- SAVAGE, C., M. HAMELIN, J. G. CULOTTI, A. COULSON, D. G. ALBERTSON *et al.*, 1989 *mec-7* is a beta-tubulin gene required for the production of 15-protofilament microtubules in *Caenorhabditis elegans*. *Genes Dev.* **3**: 870–881.
- SEGBERT, C., R. BARKUS, J. POWERS, S. STROME, W. M. SAXTON *et al.*, 2003 KLP-18, a Klp2 kinesin, is required for assembly of acentrosomal meiotic spindles in *Caenorhabditis elegans*. *Mol. Biol. Cell* **14**: 4458–4469.
- SRAYKO, M., D. W. BUSTER, O. A. BAZIRGAN, F. J. McNALLY and P. E. MAINS, 2000 MEI-1/MEI-2 katanin-like microtubule severing activity is required for *Caenorhabditis elegans* meiosis. *Genes Dev.* **14**: 1072–1084.
- SRAYKO, M., S. QUINTIN, A. SCHWAGER and A. A. HYMAN, 2003 *Caenorhabditis elegans* TAC-1 and ZYG-9 form a complex that is essential for long astral and spindle microtubules. *Curr. Biol.* **13**: 1506–1511.
- STROME, S., and W. B. WOOD, 1983 Generation of asymmetry and segregation of germ-line granules in early *C. elegans* embryos. *Cell* **35**: 15–25.
- TRINCZEK, B., J. BIERNAT, K. BAUMANN, E. M. MANDELKOW and E. MANDELKOW, 1995 Domains of tau protein, differential phosphorylation, and dynamic instability of microtubules. *Mol. Biol. Cell* **6**: 1887–1902.
- VASQUEZ, R. J., D. L. GARD and L. CASSIMERIS, 1994 XMAP from *Xenopus* eggs promotes rapid plus end assembly of microtubules and rapid microtubule polymer turnover. *J. Cell Biol.* **127**: 985–993.
- WICKS, S. R., R. T. YEH, W. R. GISH, R. H. WATERSTON and R. H. PLASTERK, 2001 Rapid gene mapping in *Caenorhabditis elegans* using a high density polymorphism map. *Nat. Genet.* **28**: 160–164.
- WILSON, P. G., and G. G. BORISY, 1997 Evolution of the multi-tubulin hypothesis. *BioEssays* **19**: 451–454.
- WRIGHT, A. J., and C. P. HUNTER, 2003 Mutations in a beta-tubulin disrupt spindle orientation and microtubule dynamics in the early *Caenorhabditis elegans* embryo. *Mol. Biol. Cell* **14**: 4512–4525.
- XIA, L., B. HAI, Y. GAO, D. BURNETTE, R. THAZHATH *et al.*, 2000 Polyglycylation of tubulin is essential and affects cell motility and division in *Tetrahymena thermophila*. *J. Cell Biol.* **149**: 1097–1106.
- XU, L., Y. WEI, J. REBOUL, P. VAGLIO, T. H. SHIN *et al.*, 2003 BTB proteins are substrate-specific adaptors in an SCF-like modular ubiquitin ligase containing CUL-3. *Nature* **425**: 316–321.
- ZETKA, M. C., and A. M. ROSE, 1992 The meiotic behavior of an inversion in *Caenorhabditis elegans*. *Genetics* **131**: 321–332.
- ZHAI, Y., P. J. KRONEBUSCH, P. M. SIMON and G. G. BORISY, 1996 Microtubule dynamics at the G2/M transition: abrupt breakdown of cytoplasmic microtubules at nuclear envelope breakdown and implications for spindle morphogenesis. *J. Cell Biol.* **135**: 201–214.

Communicating editor: A. VILLENEUVE